Modeling of the strand and mold temperature in the continuous steel caster

Z. MALINOWSKI, M. RYWOTYCKI
AGH University of Science and Technology, Al. Mickiewicza 30, 30-059 Kraków, Poland

The finite element 3D model has been developed to study the heat transfer and fluid flow in the mold region for the continuous steel casting . The strand and mold temperature is controlled by the heat transfer through steel – mold interface. The thermal resistance of interface layer has been modeled taking into consideration the convection heat transfer coefficient between the liquid steel and mold surface as an upper limit and the radiation heat transfer as an lower limit. An empirical equation has been derived to model heat conduction through the steel – mold interface. The computation has been performed to study the model response to thermal resistance of the mold –steel interface and the casting speed.

Keywords**:** *Heat transfer, fluid flow, finite element method*

1. Introduction

In steel plants, which produce the hot rolled products, steel is continuously cast in the form of slabs. It is the most efficient technology used worldwide. Solidification of steel in the mold plays fundamental role in the sheet quality. Essential developments in the design of mold and casting technology have been observed in recent years. These include on-line control of the mold oscillation and the electromagnetic stir of the liquid steel. Quality of a mold material and taper design have been improved substantially [1]. The control of heat transfer in the mold and secondary cooling zones plays an essential role in the solidification of steel. The heat exchange limits the casting speed and essentially influence the formation of the solid shell [2]. A casting machine is a heat exchanger and heat is extracted from the solidifying steel by cooling water. However, the process of heat transfer is complex. It depends on heat convection and heat conduction in the steel-slag-mold system. Kinetic energy of a liquid steel flowing from the nozzle causes mass movement and increases heat convection in the liquid region. In the mold a slag rim is formed on the plates. The thermal resistance of the slag rim and lubricant limits the heat flux transferred to the mold plates. The plates are made of copper or Cu-Ag, Cu-Cr-Zn alloys. Copper alloys improve strength and creep resistance of plates, however the conductivity is reduced. Vertical grooves are machined in plates on the side of the casing. It improves circulation of cooling water. The grooves dimensions and water velocity have direct impact on the heat transfer coefficient between cooling water and the mold plates. The described factors have

been taken into consideration in the numerical model of heat transfer in continuous casting of the square slab. The temperature fields of the mold and slab and the development of the solid shell have been analyzed.

2. The Heat and mass transfer models

2.1 Metal flow and heat transfer in the strand

The transfer of energy in the strand is composed of heat conduction in the solid shell and in the liquid core. In addition, in the liquid zone heat transfer take place by convection, which results from mass movement due to kinetic energy of pouring a molten metal into the mold [3]. Heat transfer by radiation in the liquid zone can be neglected and the strand temperature field is computed from the solution to the equation [4]:

$$\frac{\partial T}{\partial \tau} + v_x \frac{\partial T}{\partial x} + v_y \frac{\partial T}{\partial y} + v_z \frac{\partial T}{\partial z} = \frac{\lambda}{\rho c}\left(\frac{\partial^2 T}{\partial x^2} + \frac{\partial^2 T}{\partial y^2} + \frac{\partial^2 T}{\partial z^2}\right) + \frac{q_v}{\rho c} \quad (1)$$

where:
T – steel temperature, K, τ – time, s, v_x, v_y, v_z – steel velocity field, m/s, λ– thermal conductivity of steel, W/(m K), q_v– internal heat source, W/m^3, c– specific heat of steel, J/(kg K), ρ – steel density, kg/m^3, q_v – internal heat source, W/m^3

In Eq. (1) the velocity field describes movement of the liquid steel and the solid shell. The velocity field can be computed from the solution to the system of equations [5]:

$$\frac{dv_x}{d\tau} = X - \frac{1}{\rho}\frac{\partial p}{\partial x} + \frac{\mu}{\rho}\left(\frac{\partial^2 v_x}{\partial x^2} + \frac{\partial^2 v_x}{\partial y^2} + \frac{\partial^2 v_x}{\partial z^2}\right)$$

$$\frac{dv_y}{d\tau} = Y - \frac{1}{\rho}\frac{\partial p}{\partial y} + \frac{\mu}{\rho}\left(\frac{\partial^2 v_y}{\partial x^2} + \frac{\partial^2 v_y}{\partial y^2} + \frac{\partial^2 v_y}{\partial z^2}\right) \quad (2)$$

$$\frac{dv_z}{d\tau} = Z - \frac{1}{\rho}\frac{\partial p}{\partial z} + \frac{\mu}{\rho}\left(\frac{\partial^2 v_z}{\partial x^2} + \frac{\partial^2 v_z}{\partial y^2} + \frac{\partial^2 v_z}{\partial z^2}\right)$$

$$\left(\frac{\partial v_x}{\partial x} + \frac{\partial v_y}{\partial y} + \frac{\partial v_z}{\partial z}\right) = 0 \quad (3)$$

where:
p – hydrostatic pressure, Pa, X,Y,Z – mass forces, m/s^2, μ – dynamic viscosity of steel, kg/(m s),

Eq. (2) describes the motion of the steel in the control volume and Eq. (3) gives the continuity condition of the metal flow. The motion of the liquid metal and the solid shell is forced by the withdrawal constant speed and a continuous molten steel feed. Thus, it is a case of the forced steady state flow and the influence of acceleration of

gravity on the velocity field is neglected.

2.2 Boundary conditions

Solution to the general heat transfer Eq. (1) should obey the boundary conditions specified on the steel surface. In the mold, on the steel – mold interface S_{sm} heat flux q_{sm} must be equal to:

$$q_{sm} = \alpha_{sm}(T_s - T_m)\ on\ S_{sm} \quad (4)$$

where:
α_{sm} – combined heat transfer coefficient, W/(m^2 K), T_m – mold temperature, K, T_s – steel temperature, K.

Below the mold on free surface of the strand S_{sf} convection boundary condition is specified and the heat flux q_{sf} can be expressed as

$$q_{sf} = \alpha_s(T_s - T_{ws})\ on\ S_{sf} \quad (5)$$

where:
α_s – convection heat transfer coefficient for water spray cooling, W/(m^2 K).

Casting process consists of filling the mold with molten steel and its solidification. Below the meniscus level molten metal flows over the mold wall and convection is the main mechanism of heat transfer. Due to rapid cooling of the laminar layer of the liquid steel solidification starts and a gap between steel and mold is formed. For fully developed gap heat transfer mechanism changes to radiation. Thus, two boundaries for the heat transfer coefficient value can be prescribed. The upper bound is defined by the convection heat transfer coefficient α_l on the liquid steel – mold interface and the lover bound by the radiation heat transfer coefficient α_r in the gap. The value of α_r can be calculated taking into consideration radiation heat transfer between parallel plates

$$\alpha_r = 5.67\ 10^{-8}\frac{\varepsilon_s\varepsilon_m}{\varepsilon_s+\varepsilon_m-\varepsilon_s\varepsilon_m}\frac{T_s^4-T_m^4}{T_s-T_m} \quad (6)$$

where:
ε_s – emissivity of the strand surface, ε_m – emissivity of the mold surface.

Interface between mold and strand can be characterized by thermal contact conductance and the value of the heat transfer coefficient α_c is expressed by the empirical equation

$$\alpha_c = (\alpha_l - \alpha_r)exp^{\frac{T_s-T_{lt}}{200}} \quad (7)$$

where
α_l – convection heat transfer coefficient for liquid steel, W/(m^2 K)

Convection heat transfer coefficient α_l may vary from 500 to 2500 W/(m^2 K). Maximum value has been reported in [5]. The Nusselt relation due to Sleicher and Rouse [4] can be used to calculate α_l for liquid metals

$$Nu = 4.8 + 0.056 Re_s^{0.85} Pr_m^{0.93} \quad (8)$$

The Reynolds number *Re* should be evaluated at the liquid steel bulk average temperature. The casting temperature can be used instead. The subscript *m* indicates that the Prandtl number *Pr* is to be calculated at the mold surface temperature.

Below the liquidus temperature combined conduction and radiation heat transfer take place as the gap between the mold and strip develops. In this stage of solidification decreases conduction and increases radiation process. However, decrease in the strip surface temperature lids to significantly slower heat exchange. Below the solidus temperature the combined heat transfer coefficient can be expressed as

$$\alpha_{sm} = \alpha_c + \alpha_r \quad (9)$$

Typical distributions of the heat transfer coefficient are presented in Fig 1. Calculations have been performed for α_l=2000 W/(m^2 K), T_m=100 °C, ε_s=0.8, and ε_m=0.6.

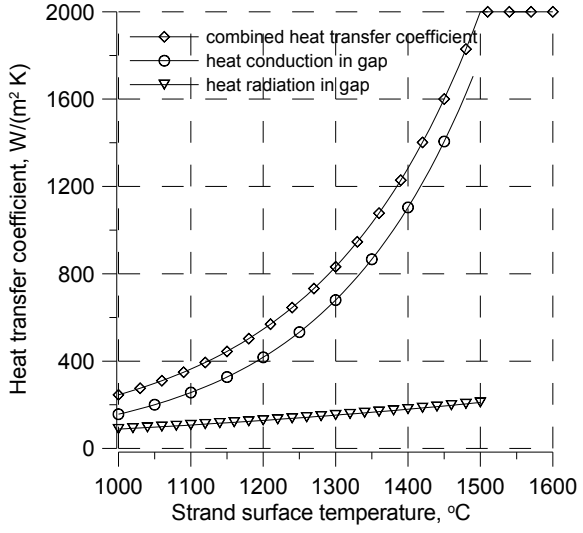

Fig. 1. Combined heat transfer coefficient on the steel – mold interface as a function of the strand temperature for α_l=2000 W/(m^2 K), T_m=100 °C, ε_s=0.8, and ε_m=0.6.

Outside the mold, strand is cooled by water sprays and the convection heat transfer

coefficient α_s can be calculated from [6]:

$$\alpha_s = 10^9\ 3.15\ \dot{w}^{0.616}\left[700 + \frac{t-700}{exp(0.1t-70)+1}\right]^{-2.455}\left[1 - \frac{1}{exp(0.025t-6.25)+1}\right] \quad (10)$$

where:
t – strand surface temperature, °C, $\dot{w}$ – water spray flux rate, dm^3/(m^2 s).

Presented in Fig. 2 variation of the heat transfer coefficient as a function of strand temperature is typical for water cooling. For the water spray flux rate $\dot{w}$ = 3 dm^3/(m^2 s) and the strand surface temperature t = 700°C the heat transfer coefficient α_s = 650 W/(m^2 K). Similar values of heat transfer coefficient for water spray cooling has been reported in [7]. Meniscus surface temperature has been set equal to casting temperature T_{in} = 1790 K.

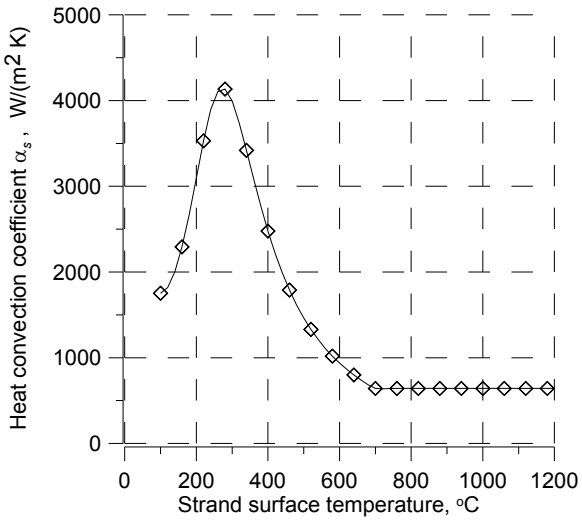

Fig. 2. Distribution of the heat convection coefficient as a function of the strand surface temperature for the water spray flux rate $\dot{w}$ = 3 dm^3/(m^2 s)

Scheme of kinematical boundary condition for flow analysis has been presented in Fig. 3. On free surface of the liquid steel two zones can be determined. In the first zone, which simulates the charging nozzle, normal velocity v_z is equal to pouring velocity v_{in} and tangent velocity v_x=0. For the second zone the slip wall condition has been adopted and normal velocity v_z is set to zero. On the steel - mold interface the slip wall condition has been assumed and velocity v_x is set to zero, furthermore for the solid shell v_z equal to casting speed v_c is set. In the cross section of the strand below the mold for the solid shell v_x=0 and v_x= v_c have been prescribed and for the liquid steel only v_x=0 has been assumed.

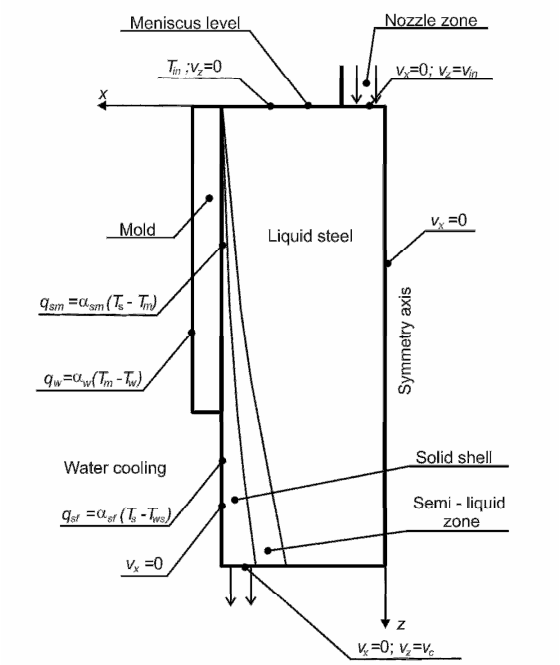

Fig. 3. Scheme of the continuous casting process and the boundary conditions for steel flow and heat transfer models**.**

2.3 The mold temperature model

Determination of the strand temperature field requires knowledge of the mold surface temperature T_s. Its value can be defined if the mold temperature field is known. The mold temperature field can be determined from the solution to the three dimensional heat transfer equation

$$\frac{\partial T}{\partial \tau} = \frac{\lambda}{\rho c}\left(\frac{\partial^2 T}{\partial x^2} + \frac{\partial^2 T}{\partial y^2} + \frac{\partial^2 T}{\partial z^2}\right) \tag{11}$$

The mold is taking heat from the strand and is simultaneously water cooled on the outside surface. On the inner surface of mold the boundary condition has the form

$$q_{sm} = \alpha_{sm}(T_s - T_m)\ on\ S_{sm} \tag{12}$$

The heat transfer coefficient α_{sm} is defined in the same way as for the strand temperature model. Outer surface of the mold is water cooled and the heat flux is given by

$$q_w = \alpha_w(T_m - T_w)\ on\ S_{sw} \tag{13}$$

where:
α_w – is the heat transfer coefficient for water cooling in mold channels, W/(m^2 K), T_w – cooling water temperature, K.

Water cooling channels are machined in mold in a form of grooves of a side length 3 to 5 mm. Most relation for the heat transfer coefficient for turbulent flow are based on experimental studies. The Nusselt number relation due to Michiejew [8] can be used

$$Nu = 0.021 Re_w^{0.8} Pr_w^{0.43} \left(\frac{Pr_w}{Pr_s}\right)^{0.25} \quad (14)$$

Subscript *s* indicates that the Prandtl number *Pr* must be evaluated at the mold surface temperature and subscript *w* denotes that the Reynolds *Re* and Prandtl *Pr* numbers are to be evaluated at the mean bulk temperature of water. Once the Nusselt number is known the convection heat transfer coefficient for water cooling is determined from

$$\alpha_w = \frac{Nu\lambda_w}{D_h} \quad (15)$$

where:
D_h – hydraulic diameter of the water cooling channel, m, λ_w – water conductivity, W/(m K).

Several mold cooling strategies can be obtained varying the grooves dimensions and the distance between grooves [9].

2 Results and dyscusion

Finite element method has been chosen to solve the heat transfer and metal flow problems [3, 10]. Computer code have been developed to simulate the temperature and velocity fields in the continues steel caster. Computations have been performed for the mold of 160mm×160mm cross section and 700mm long. The mold corner radius has been assumed equal to 15mm. Further, it has been assumed that mold is made of Cu-Ag alloy and cooling grooves with hydraulic diameter D_h=4mm are evenly distributed over the outer mold surface. Physical parameters of the mold material and cooling water are listed in Table 1.

Table 1. Physical properties of the mold material [1,4] and cooling water [4] at room temperature.

Material	Thermal conductivity W/(m K)	Density kg /m^3	Specific heat J/(kg K)
Water	0.607	997	4180
Cu-Ag alloy	370	8900	400

The simulations have been performed for the bulk average velocity of cooling water v_w=4.5m/s. Chemical composition and properties of carbon steel used in computations

are listed in Table 2 and Table 3, respectively.

Table 2. Chemical composition of the carbon steel used in simulation

Element	C	Si	Mn	P	S
wt %	0.35	0.20	0.75	0.04	0.04

Table 3. Physical properties of the carbon steel used in simulation

Property	Unit	Value or function of temperature
Liquidus temperature [14]	^{o}C	1500
Solidus Temperature [14]	^{o}C	1460
Heat of solidification [11]	J/m^3	10^9 1.93
Dynamic viscosity – liquid [12]	kg/(m s)	0.00285
Thermal conductivity – liquid [11]	W/(m K)	35
Density – liquid [13]	kg/m^3	$\rho = \frac{1}{0.1235 + 12.67 * 10^{-6} T + 9 * 10^{-2} C}$
Specific heat – liquid [11]	J/(kg K)	574
Thermal conductivity – austenite [10]	W/(m K)	14.24+0.0127 t
Density – austenite [13]	kg/m^3	$\rho = \frac{1}{0.1235 + 9.7 * 10^{-6} T + 0.4 * 10^{-2} C + 2 * 10^{-2} C^2}$
Specific heat – austenite [10]	J/(kg K)	647.522+0.005852 t

Due to symmetry of the problem finite element simulations have been limited to ¼ of the steel – mold cross section. Finite element mesh of 3136 elements for steel temperature computation has been employed. In the case of mold temperature 855 elements have been used. The example of the finite element mesh is presented in Fig. 4. For the velocity field computation 480 elements have been used in the longitudinal cross section of the strand. The steady state velocity field has been computed every 50th increment of the heat transfer solution. Since the heat transfer problem should converge to a steady state solution the coupled problem has been solved iteratively. The computations of the strand temperature field have been performed as long as the difference between the current and previous temperature field was greater than the prescribed accuracy. Usually from 2000 to 5000 time increments ware needed to reach the steady state solution.

2.1 Cooling conditions analysis

The influence of the heat transfer from the strand surface on the steel temperature and velocity fields has been analyzed. In the strand temperature model there are two parameters which can be used to study this problem. The first one is the heat convection coefficient α_l and the second one is the water spray flux rate $\dot{w}$. In order to analyze heat transfer through steel – mold interface the computations have been performed for the cases of: α_l = 1000, α_l = 1500, α_l = 2000 W/(m^2 K) and

$\dot{w}$ = 3 dm^3/(m^2 s). The water spray flux influence on the solidification process below the mold has been analyzed for the cases of: $\dot{w}$=3, $\dot{w}$=5, $\dot{w}$=10 dm^3/(m^2 s) and α_l = 2000 W/(m^2 K).The casting speed v_c = 1.5 m/min has been assumed in both cases.

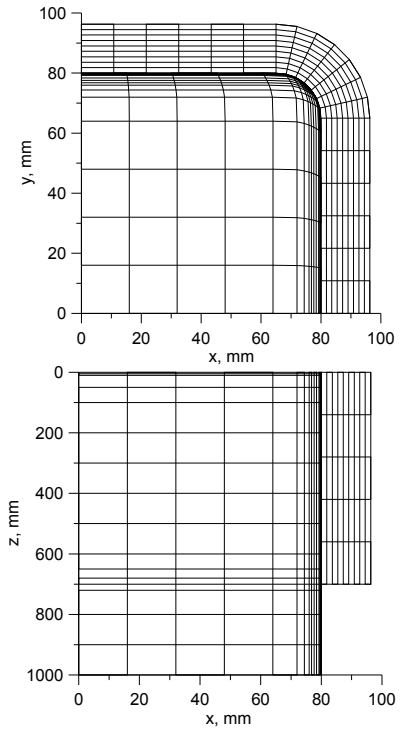

Fig. 4. The finite element mesh employed for heat transfer analysis.

Thermal resistance of the mold - steel interface on the mold and strand temperature fields in the longitudinal section are presented in Fig. 5.

Faster heat transfer through steel – mold interface results in significantly higher mold temperature. The maximum mold temperature rises to 250 ^{o}C in the zone of contact with the liquid steel. It limits further reduction of the thermal resistance of the mold – steel interface. The solid shell thickness is the highest for α_l = 2000 W/(m^2 K) and is equal to 17 mm. For the heat transfer coefficient α_l = 1000 W/(m^2 K) the solid shell thickness is 13.5 mm below the mold edge. The thermal resistance of the mold – steel interface has significant influence on the strand surface temperature. The results are shown in Fig. 6. Below the mold edge the surface temperature in the middle of the strand side drops to 1250 ^{o}C for α_l = 1000 W/(m^2 K) and to 1170 ^{o}C for α_l = 2000 W/(m^2 K). Thus, thermal resistance of the mold – steel interface can be used to control the solidification process.

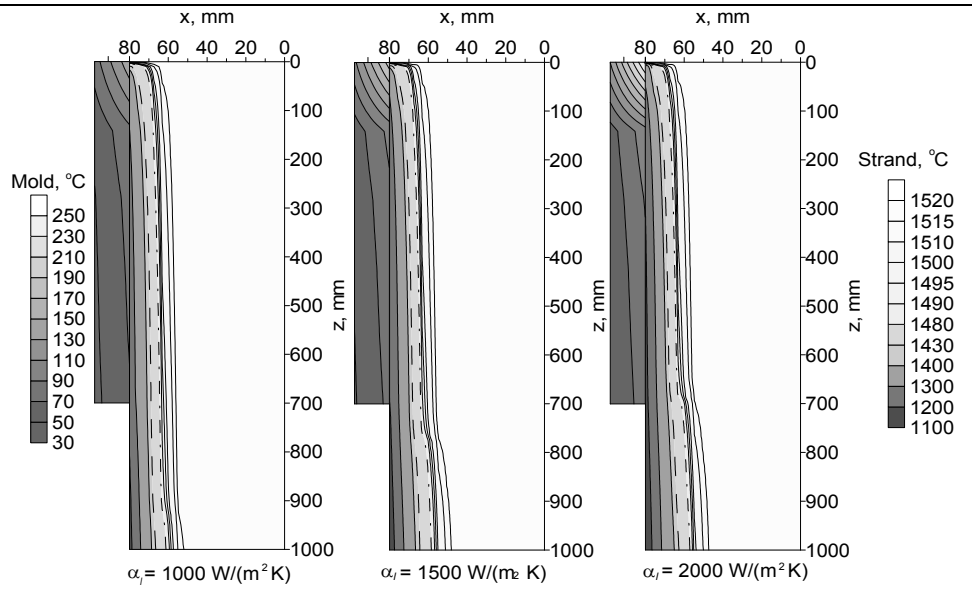

Fig. 5. The mold and strand temperature fields for various thermal resistance of the mold - steel interface.

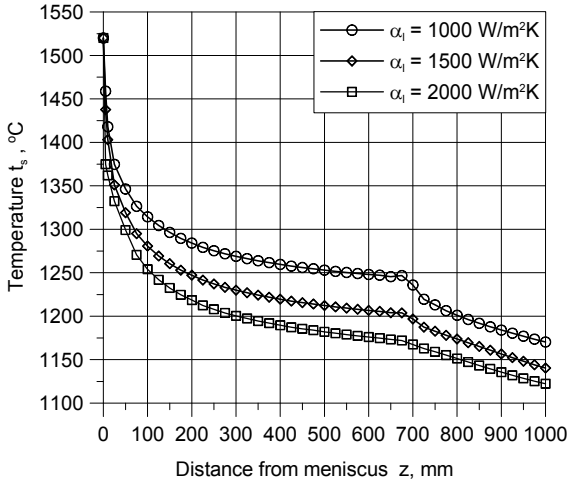

Fig. 6. The surface temperature variation in the middle of the strand side for various thermal resistance of the mold - steel interface.

The mold temperature fields for various thermal resistance of the mold – steel interface have been presented in Fig. 5 and Fig. 7.

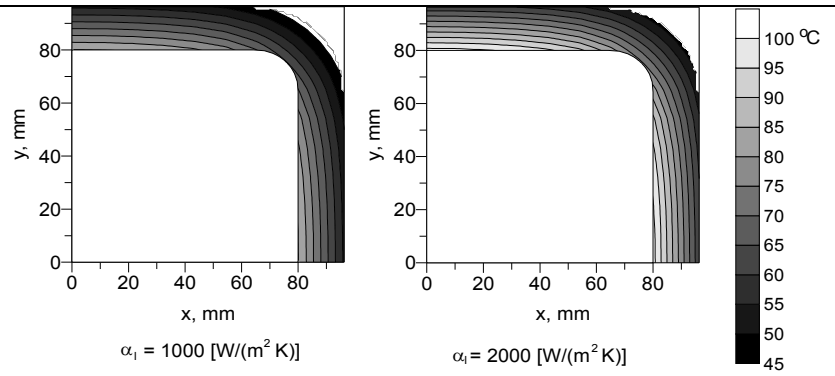

Fig. 7. The mold temperature fields in the cross 140 mm below the meniscus for various thermal resistance of the mold - steel interface

The highest mold temperature is observed at surface which is in contact with the liquid steel. The mold surface temperature drops as the gap develops in the flow direction. In the mold cross section the temperature distribution is les or more uniform with the lowest values at the mold corner. Even distribution of cooling channels over the outer mold surface results in uniform heat transfer to the cooling water. Other cooling schemes are possible in order to control the mold temperature [9]. It has been shown that the thickness of the solid shell can be controlled by the convection heat transfer coefficient which is directly related to liquid steel flow down the mold. Simple empirical equation has been developed to describe the combined heat transfer at the mold – steel interface. This equation can be easily adopted to a particular casting machine if the results of mold thermal monitoring are known. Below the mold, the strand temperature can be controlled by the water sprays applied to the strand surface. The effect of the water spray flux rate on the strand temperature is further explored in simulation, which has been performed for α_l = 2000 W/(m^2 K), casting speed v_c = 1.5 m/min and the water spray flux rates: $\dot{w}$=3, $\dot{w}$=5, $\dot{w}$=10 dm^3/(m^2 s). The results are shown in Fig. 8. The model is sensitive to the water spray cooling. The strand temperature drops significantly below the mold while along the mold the temperature remains constant. The solid shell thickness increases from 17 mm for $\dot{w}$ =3 dm^3/(m^2 s) to 19 mm for $\dot{w}$ = 10 dm^3/(m^2 s), respectively.

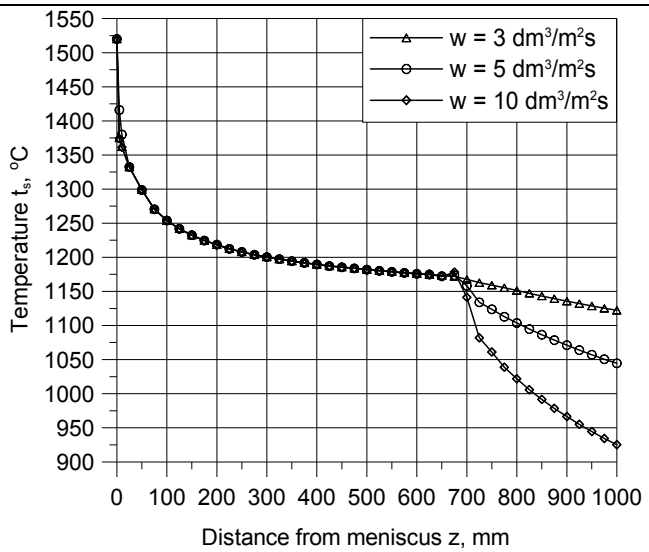

Fig. 8. The surface temperature variation in the middle of the strand side for various water spray flux rates.

2.2 Casting speed analysis

The casting speed influence on the steel solidification has been analyzed for the thermal resistance of the mold – steel interface characterized by the convection heat transfer α_l = 1500 W/(m^2 K) and the water spray flux rate in the secondary cooling chamber $\dot{w}$ = 3 dm^3/(m^2 s). The computation has been performed for the casting speed varying from 1.5 to 3.5 m/min at intervals of 0.5 m/min. The mold and strand temperature fields are presented in Fig. 9. Increase in the casting speed lids to a shorter cooling time and in consequence the strand temperature rises. In Fig. 10 variation of the strand temperature in the middle of the strand side are shown. Below the mold the strand surface temperature rises by about 50 °C as the casting speed is increased from 1.5 to 3.5 m/min. The thickness of the solid shell decreases from 16 mm for the lowest casting speed to 9.5 mm for the highest casting speed. Significant reduction of the solid shell thickness may lead to surface defects such as cracks or folding back of the solidified rim. The simulations has shown significant influence of the velocity field on the strand temperature. The heat transfer and fluid flow problems are highly coupled and stationary results can be obtained after substantial increase in the computation time.

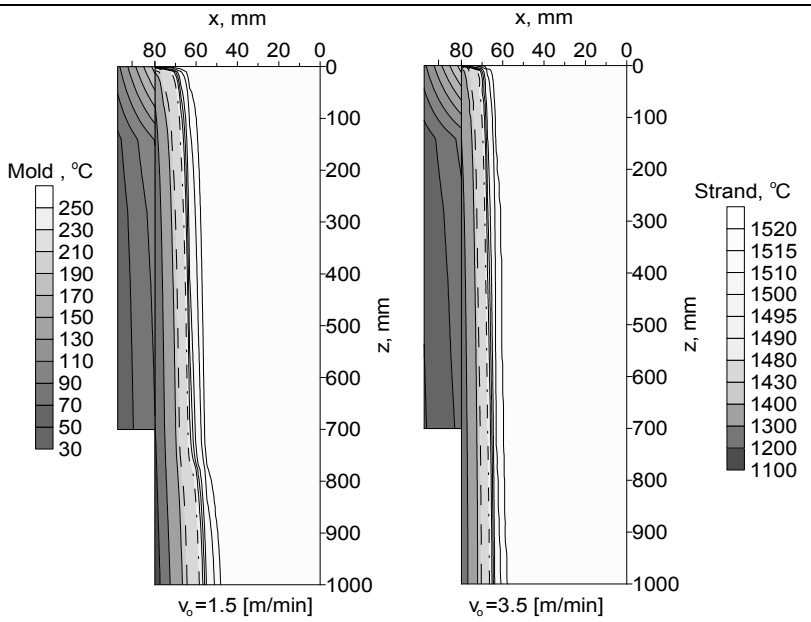

Fig. 9. The mold and strand temperature fields for the casting speed v_c = 1,5 m/min and v_c = 3,5 m/min

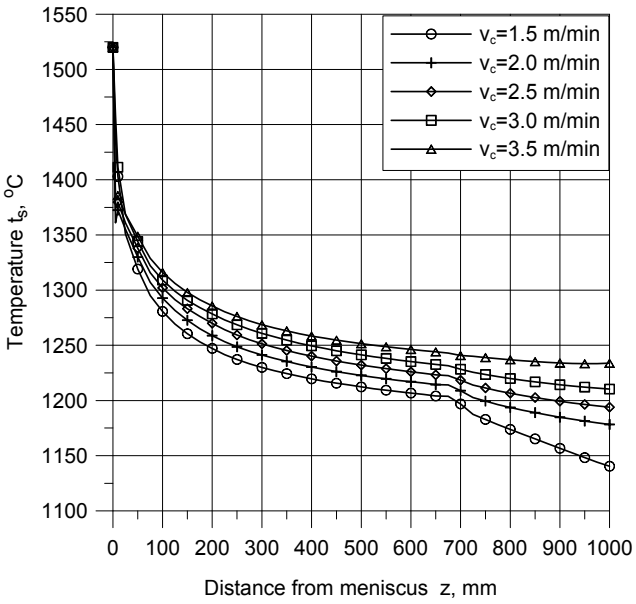

Fig. 10. The surface temperature variation in the middle of the strand side for various casting speeds

The temperature fields in the mold cross section 140 mm below the meniscus are presented in Fig. 11. The mold temperature rises as the casting speed increases. The results confirm good predictive ability of the developed mold temperature model. The mold temperature rise is caused by a higher strand surface temperature and the heat flax increase. The maximum mold temperature rises by about 15°C as the casting speed increases from 1.5 to 3.5 m/min.

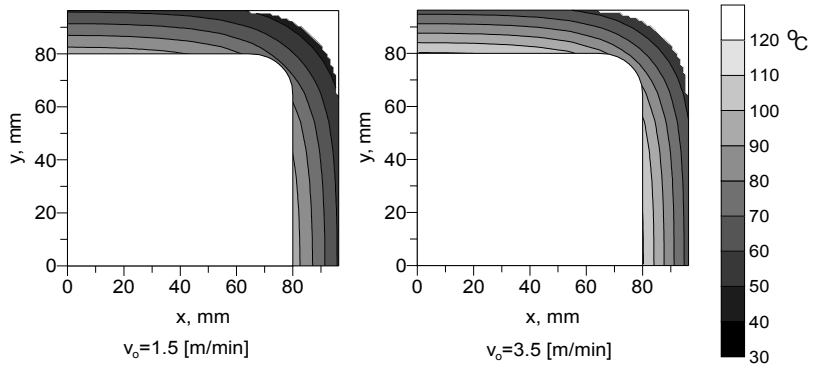

Fig. 11. The mold temperature fields in the cross section 140 mm below the meniscus for the casting speed v_c = 1,5 m/min and v_c = 3,5 m/min

3 Conclusions

In the literature several solutions to the solidification of steel in the mold region has been published. However, the problem is not well understood. The main difficulties are concerned with the description of the heat transfer through the steel – mold interface and with the determination of fluid flow. The heat transfer and fluid flow problems are highly coupled and heat convection in the liquid region makes serious problems while the temperature field is computed. The solution should converge to a steady state and only at this stage it can be assumed as the final one. Negligence of heat convection may cause essential inaccuracy in the strand temperature field. In consequence the steel solidification and formation of the solid shell is predicted with low accuracy. The empirical equation has been derived to solve the heat transfer problem through the steel – mold interface. The upper limit of the heat transfer coefficient has been determined based on the heat convection by the liquid steel flowing down the mold. The lower limit for the heat transfer coefficient sets the heat radiation in the gap. The computations have shown good response of the finite element solution to the thermal resistance of the steel – mold interface, water spray cooling in the secondary chamber and to the casting speed. Predictions of the finite element 3D model are consistent with results published in the literature. Further effort has to be done in order to limit the computation time and to improve description of the boundary conditions.

Acknowledgements

The work has been supported by the Ministry of Science and Higher Education Grant No N R07 0018 04

4 Literature

[1] S. Normanton, P. Watson, N. Hardwick: Some developments in mould technology. In: Proc. 3rd European Conference on Continuous Casting, Madrid, 1998, 737-743.

[2] J.A Dilellio., G.W.Young: An asymptotic model of the mould region in continuous steel caster. Metallurgical Transactions. 26 (1995), 1225-1241.

[3] M. Rywotycki, Z. Malinowski: Modeling of fluid flow in the steel continuous casting process. Metallurgy and Foundry Engineering, 30 (2004), 99–108.

[4] Y. A. Çengel: Heat and Mass Transfer: a practical approach. McGraw-Hill, New York, 2007

[5] J. Malczewski, M. Piekarski: Modele procesów transportu masy pędu i energii. PWN, Warszawa, 1992.

[6] P. D. Hodgson, K.M. Browne,. D.C. Collinson, T.T. Pham, R.K Gibbs: A mathematical model to simulate the thermo-mechanical processing of steel. In: Proc. 3rd Int. Seminar of the International Federation for Heat Treatment and surface Engineering, Melbourne, 1991, 139-159.

[7] J. K. Park, B. G. Thomas, I. V. Samarasekera: Analysis of thermo mechanical behaviour in billet casting with different mold corner radii. Ironmaking and Steelmaking, 29 (2002), 359-375.

[8] S. Wiśniewski, T.S. Wiśniewski: Wymiana ciepła, WNT, Warszawa, 1994.

[9] M. Rywotycki, Z. Malinowski, T. Telejko: Wpływ konstrukcji krystalizatora na pole temperatury pasma COS. Hutnik - Wiadomości Hutnicze, 4 (2006), 142–147.

[10] Z. Malinowski: Numeryczne modele w przeróbce plastycznej i wymianie ciepła. UWND AGH, Kraków, 2005.

[11] W. Kurz, D.J. Fisher: Fundamentals of Solidification, Trans. Tech. Publications, Switzerland, 1998.

[12] G. Kniaginin: Staliwo - Metalurgia i Odlewnictwo. Śląsk, Katowice, 1972.

[13] J. Theret, G. Lesoult: Deroulement de la solidification des fonts a graphite spheroidal. Hommes et Fonderie, Fevrier, 4 (1984), 19 – 30.

[14] G. Beranger, G. Henry, G. Sanz: The Book of Steel, Intercept Ltd, New York, 1996.

	Modelowanie pola temperatury pasma i krystalizatora COS W pracy przedstawiono model numeryczny opisujący wymianę ciepła pomiędzy krystalizatorem a pasmem w procesie ciągłego odlewania stali. Analizie poddano wpływ warunków wymiany ciepła w obszarze krystalizatora na pole temperatury pasma. Wykonano obliczenia pozwalające ocenić wpływ prędkości odlewania na pole temperatury krystalizatora i pasma. Zadanie rozwiązano z zastosowaniem metody elementów skończonych.